TOWARDS FLUID SIMULATIONS OF DISPERSIVE MHD WAVES IN A WARM COLLISIONLESS PLASMA

G. Bugnon, R. Goswami, T. Passot and P.L. Sulem [1]

[1] *CNRS, Observatoire de la Côte d'Azur, B.P. 4229, 06304 Nice Cedex 4, France*

ABSTRACT

A Landau fluid model suited for the description of the weakly nonlinear dynamics of long wavelength dispersive MHD waves in a magnetized collisionless plasma is presented, that should be useful to study the formation and stability of solitary structures such as magnetic holes or shocklets observed for example in the solar wind and the terrestrial magnetosheath. First simulations in a slab geometry are reported, that focus on the evolution of plane fast magnetosonic waves. Accurate comparisons are made with analytic predictions of the Landau damping rate for various plasma parameters and wave characteristics. In a regime where Landau damping dominates, Alfvén modes eventually become prevalent, which results in the arrest of dissipation at a time that is shorter for waves with larger initial amplitude. In contrast, magnetosonic solitary waves in the form of density and magnetic field depressions are found to emerge in a regime where Landau dissipation is initially negligible compared with nonlinear and dispersive effects. Excellent agreement is also found for the growth rate of the mirror instability at long wavelength but modeling the arrest of the instability at small scales within fluid simulations remains a challenging issue.

INTRODUCTION

Both in natural and fusion plasmas, collisions are generally negligible and kinetic effects relevant. On the other hand, when a broad range of scales is involved, direct numerical integrations of the Vlasov-Maxwell equations in three space dimensions are beyond the capabilities of the present day computers. Such situations actually require a formalism that preserves most of the aspects of a fluid description but extends the usual magnetohydrodynamics by including realistic approximations of the pressure and heat flux tensors. Wave-particle resonances present at the hydrodynamical scales (Landau damping) provide an important dissipation and should thus be retained. Such a description turns out to be possible for a plasma permeated by a strong ambient magnetic field. In this context, Snyder *et al.* (1997) suggested a "Landau fluid" model involving hydrodynamic equations for the density and the velocity of the plasma, together with dynamical equations for the parallel and perpendicular pressures of each species. The resulting system must nevertheless be closed and the main issue consists in a proper determination of the heat fluxes that enter the pressure equations. For the sake of simplicity, an electron-proton plasma is considered in a simple geometry (no curvature drift), with an homogeneous equilibrium state characterized by bi-Maxwellian distribution functions. In the original formulation, the model is limited to scales large enough for both Hall effect and finite Larmor radius corrections to be negligible. A generalization is needed in order to account for dispersive effects. For this purpose, the derivation was revisited by Passot and Sulem (2004b) who extended this mono-fluid model in a form able to accurately reproduce the weakly nonlinear dynamics of dispersive MHD waves for any β larger than the electron to proton mass ratio m_e/m_p and any propagation angle α (thus including kinetic Alfvén waves with a transverse wavenumber small compared with the inverse proton inertial length). This model is expected to provide an efficient tool to investigate the presence of coherent structures in the form of solitary waves such as magnetic holes, shocklets or oscillitons reported by satellite observations in the solar wind and the terrestrial magnetosheath. Such structures are classically understood as resulting from a balance between dispersion and nonlinearity, but their persistence in regimes where Landau damping and coupling to other waves are relevant remains to be understood. Long-wave asymptotics can be performed from Landau fluid models and lead to soliton equations, possibly perturbed by weak Landau damping (Passot and Sulem, 2004a), but the question remains to determine the regimes where the formation of solitary structures is not hampered by other phenomena.

THE MODEL AND ITS VALIDATION

The Landau fluid model for dispersive MHD waves derived in Passot and Sulem (2004b) is briefly described in the Appendix. Here, we concentrate on a simplified version that is sufficient in the case of magnetosonic waves and was also shown to accurately reproduce the parallel Alfvén wave dynamics (Passot and Sulem, 2003). It consists in retaining only the leading order non-gyrotropic contributions to the pressure tensors and also neglecting both the non-gyrotropic corrections to the heat flux tensors and the corrections to the gyrotropic components due to parallel current. In a slab geometry, where the ambient magnetic field makes an angle α with the direction of propagation (denoted by x), the equations obeyed by the density ρ (measured in units of the equilibrium value $\rho^{(0)}$), the plasma velocity (u_x, u_y, u_z) (taken in units of a velocity u_0 that we will take as the Alfvén velocity v_A), the magnetic field $(b_x = B_0 \cos\alpha, b_y, b_z)$ (measured in units of the ambient field B_0), the parallel and perpendicular pressures $p_{\|r}$ and $p_{\perp r}$ (both measured in units of the equilibrium parallel proton pressure $p_0 = p_{\|p}^{(0)}$) and heat fluxes $q_{\|r}$ and $q_{\perp r}$ of each species (taken in units of $u_0 p_0$), read

$$\partial_t \rho + \partial_x(\rho u_x) = 0 \tag{1}$$

$$\partial_t u_x + u_x \partial_x u_x + \frac{\beta}{2M_a^2}\frac{1}{\rho}\partial_x(p_{xx} + \pi_{xx}) + \frac{1}{M_a^2}\frac{1}{\rho}\partial_x \frac{|b|^2}{2} = 0 \tag{2}$$

$$\partial_t u_y + u_x \partial_x u_y + \frac{\beta}{2M_a^2}\frac{1}{\rho}\partial_x(p_{xy} + \pi_{xy}) - \frac{b_x}{M_a^2}\frac{1}{\rho}\partial_x b_y = 0 \tag{3}$$

$$\partial_t u_z + u_x \partial_x u_z + \frac{\beta}{2M_a^2}\frac{1}{\rho}\partial_x(p_{xz} + \pi_{xz}) - \frac{b_x}{M_a^2}\frac{1}{\rho}\partial_x b_z = 0 \tag{4}$$

$$\partial_t b_y = \partial_x\Big(b_x u_y - u_x b_y + \frac{R_p b_x}{M_a}\frac{\partial_x b_z}{\rho} - \frac{\beta}{2}\frac{R_p}{M_a}\frac{1}{\rho}\partial_x p_{e,xz}\Big) \tag{5}$$

$$\partial_t b_z = \partial_x\Big(b_x u_z - u_x b_z - \frac{R_p b_x}{M_a}\frac{\partial_x b_y}{\rho} + \frac{\beta}{2}\frac{R_p}{M_a}\frac{1}{\rho}\partial_x p_{e,xy}\Big) \tag{6}$$

$$\partial_t p_{\|r} + \partial_x(u_x p_{\|r}) + 2\frac{p_{\|r}}{|b|^2}(b_x^2\partial_x u_x + b_x b_y \partial_x u_y + b_x b_z \partial_x u_z) + \partial_x\Big(\frac{b_x}{|b|}q_{\|r}\Big) - 2q_{\perp r}\partial_x \frac{b_x}{|b|} = 0 \tag{7}$$

$$\begin{aligned}\partial_t p_{\perp r} + \partial_x(u_x p_{\perp r}) + p_{\perp r}\partial_x u_x - \frac{p_{\perp r}}{|b|^2}(b_x^2\partial_x u_x + b_x b_y \partial_x u_y + b_x b_z \partial_x u_z)&\\ +\partial_x\Big(\frac{b_x}{|b|}q_{\perp r}\Big) + q_{\perp r}\partial_x\frac{b_x}{|b|} = 0&\end{aligned} \tag{8}$$

$$\Big(\partial_t + u_x\partial_x + \frac{1}{\left(\frac{u_0}{v_{th,r}}\right)}\frac{\cos\alpha}{\sqrt{\frac{8}{\pi}}\left(1-\frac{3\pi}{8}\right)}\mathcal{H}\partial_x\Big)q_{\|r} = \frac{\cos\alpha}{\left(\frac{u_0^2}{v_{th,r}^2}\right)\left(1-\frac{3\pi}{8}\right)}\partial_x\Big(\frac{p_{\|r}}{\rho}\Big) \tag{9}$$

$$\Big(\partial_t + u_x\partial_x - \frac{1}{\left(\frac{u_0}{v_{th,r}}\right)}\cos\alpha\sqrt{\frac{\pi}{2}}\mathcal{H}\partial_x\Big)q_{\perp r} = -\frac{\cos\alpha}{\left(\frac{u_0^2}{v_{th,r}^2}\right)}\partial_x\Big[\frac{p_{\perp r}}{\rho} + \Big(\frac{p_{\perp r}^{(0)}}{p_{\|r}^{(0)}} - 1\Big)\frac{p_{\perp r}^{(0)}}{p_0}|b|\Big], \tag{10}$$

where the gyrotropic components of the pressure tensor are given by $p_{ij} = \sum_r p_{r,ij}$ with

$$p_{r,xx} = p_{\perp r} + (p_{\| r} - p_{\perp r})\frac{b_x^2}{|b|^2} \tag{11}$$

$$p_{r,xy} = (p_{\| r} - p_{\perp r})\frac{b_x b_y}{|b|^2} \tag{12}$$

$$p_{r,xz} = (p_{\| r} - p_{\perp r})\frac{b_x b_z}{|b|^2}. \tag{13}$$

In these equations, $\mathcal{H}$ denotes the Hilbert transform relatively to the x coordinate, $v_{thr} = \sqrt{\frac{T^{(0)}_{\| r}}{m_r}}$ is the thermal velocity of the particles of species r, $M_a = \frac{u_0}{v_A}$ is the Alfvénic Mach number (here taken equal to 1) and $\beta = \frac{8\pi p_0}{B_0^2}$. Neglecting the electron-proton mass ratio, one gets $\frac{u_0^2}{v_{th,p}^2} = \frac{2M_a^2}{\beta}$ and $\frac{u_0^2}{v_{th,e}^2} = 2\frac{m_e}{m_p}\frac{p^{(0)}_{\| p}}{p^{(0)}_{\| e}}\frac{M_a^2}{\beta}$. Furthermore, $R_p = \frac{v_A}{\Omega_p L_0}$ where $\Omega_p = \frac{eB_0}{m_p c}$ measures the ratio of the protons inertial length to the considered length scale L_0. The non-gyrotropic corrections in the pressure tensor are restricted to their leading order in the form

$$\pi_{xx} = M_a R_p \sin\alpha\Big(2\cos^2\alpha(p_{\perp p} - 2p_{\| p}) - \frac{1}{2}\sin^2\alpha p_{\perp p}\Big)\partial_x u_y \tag{14}$$

$$\begin{aligned}\pi_{xy} = {} & M_a R_p \cos\alpha\Big((p_{\perp p} - 2p_{\| p}\cos^2\alpha)\partial_x u_z + 2p_{\| p}\cos\alpha\sin\alpha\partial_x u_x\Big) \\ & + M_a R_p \sin^2\alpha p_{\perp p}(\sin\alpha\partial_x u_x - \cos\alpha\partial_x u_z)\end{aligned} \tag{15}$$

$$\pi_{xz} = M_a R_p \cos\alpha\Big((\sin^2\alpha - \cos^2\alpha)(p_{\perp p} - 2p_{\| p}) + \sin^2\alpha p_{\perp p}\Big)\partial_x u_y. \tag{16}$$

LANDAU DAMPING OF MAGNETOSONIC WAVES

The rate $\lambda_I k v_A$ of Landau dissipation for an oblique magnetosonic wave of wave number k propagating in a plasma with isotropic equilibrium temperatures simply expresses in the case $\frac{m_e}{m_p} \ll \beta \ll \frac{T_e}{T_p}$ with $\beta \ll 1$ where (Passot and Sulem, 2004a)

$$\lambda_I = -\sqrt{\beta}\sqrt{\frac{\pi}{8}}\sqrt{\frac{m_e}{m_p}}\frac{\sin^2\alpha}{\cos\alpha}\Big[1 + \frac{2\beta^2\cos^4\alpha}{(1+\beta-2\beta\cos^2\alpha)\lambda_R^2 - \beta\cos^2\alpha}\Big], \tag{17}$$

with a phase velocity $\lambda_R v_A$ given by

$$\lambda_R^2 = \frac{1+\beta \pm \sqrt{(1+\beta)^2 - 4\beta\cos^2\alpha}}{2}. \tag{18}$$

We here concentrate on the case of fast waves (associated with the positive sign) for which Landau dissipation is usually weaker. In order to approach the asymptotic regime addressed by the theory, we choose a temperature ratio $T_e/T_p = 10$, and prescribe small values for the parameter β.

Simulations were performed using a Fourier spectral method in a 2π periodic domain, with a resolution of 128 or 256 collocation points. The initial conditions are taken in the form of a pure magnetosonic wave. Defining $A = a_0 \cos kx$ and $\rho^{(1)} = \rho - \rho^{(0)} = RA$, where the constant R is given by Eq. (26) of Passot and

Sulem (2004b) with the quantities $\mathcal{C}_{\|}$ and $\mathcal{C}_{\perp}$ approximated by $\sqrt{\beta}v_A$, we prescribe as initial conditions $b_y = 0$, $b_z = B_0 \sin\alpha + \dfrac{A}{\sin\alpha}$, $u_x = \lambda_R \rho^{(1)}$, $u_z = \lambda_R \tan\alpha \rho^{(1)} - \dfrac{\lambda_R}{\sin\alpha\cos\alpha} A$, together with $q_{\|e} = 2\dfrac{\lambda_R}{\cos\alpha}(A - \rho^{(1)})$, $q_{\perp e} = \dfrac{\lambda_R}{\cos\alpha}(A - \rho^{(1)})$ and $q_{\|p} = q_{\perp p} = 0$. Note that this initial condition induces an mean contribution to u_z.

β	Analytical value	Numerical results
10^{-1}	-0.007518	-0.007605
$4.\ 10^{-2}$	-0.004763	-0.004777
10^{-2}	-0.002382	-0.002403
$2.5\ 10^{-3}$	-0.001191	-0.001228
10^{-3}	-0.000753	-0.000791

$\cos\alpha$	Analytical value	Numerical results
0.2	-0.015696	-0.016606
0.5	-0.004904	-0.004991
0.7	-0.002382	-0.002403
0.85	-0.001068	-0.001073

Comparisons of the damping coefficient λ_I as given by the theory and by the numerics are presented in Table 1 where $\cos\alpha = 0.7$ and β is varied, and in Table 2 where $\beta = 10^{-2}$ and $\cos\alpha$ varied. In these simulations $R_p = 10^{-2}$ and the initial conditions are characterized by an amplitude $a_0 = 10^{-4}$. An agreement of the order of one percent is obtained in the regime where β, although small, is such that dissipation dominates the dynamics.

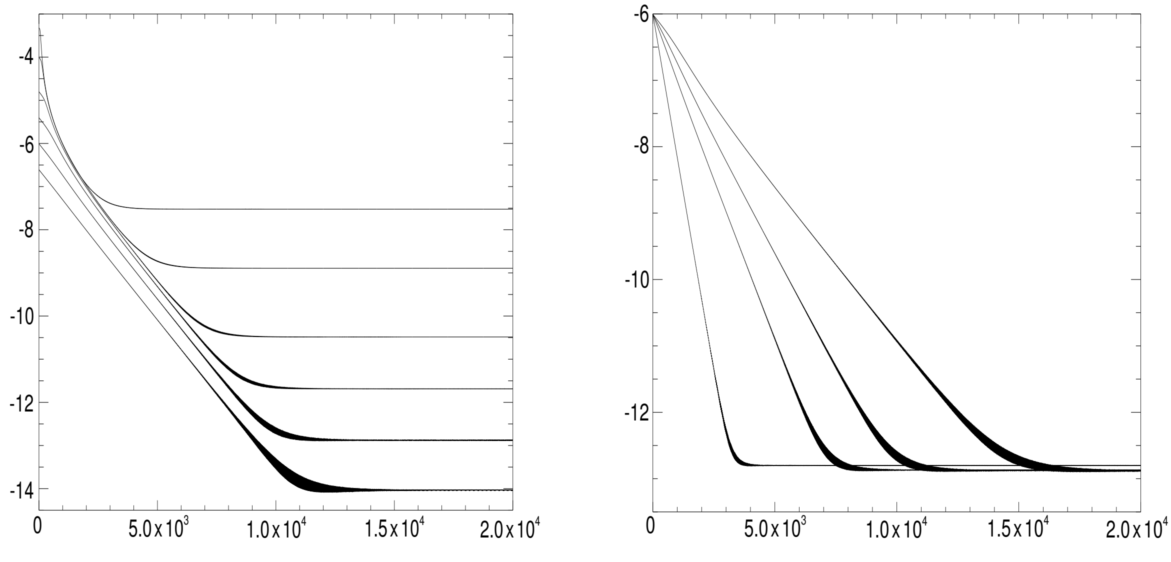

Fig. 1. Time evolution (in lin-log scales) of magnetosonic wave energy $\frac{1}{2}\int[\rho(u_x^2 + \tilde{u}_z^2) + (b_z - B_0 \sin\alpha)^2]dx$, assuming $R_p = 7.\ 10^{-3}$: (left) for initial amplitudes (from top to bottom) $a_0 = 2.210^{-2}$, 10^{-2}, 4.10^{-3}, 2.10^{-3}, 10^{-3} and 5.10^{-4}, when $\beta = 10^{-2}$; (right) for $\beta = 0.1$, 0.02, 0.01 and 0.005 (from left to right), in the case of an initial amplitude equal to $a_0 = 10^{-3}$.

LONG TIME EVOLUTION OF A MAGNETOSONIC WAVE

In order to address the dynamics beyond the linear theory, we prescribed $R_p = 7.\ 10^{-3}$ together with a propagation angle defined by $\cos\alpha = 0.7$ and performed several simulations for amplitudes a_0 ranging from 10^{-3} to $2.\ 10^{-2}$. The resulting time evolution of the magnetosonic wave energy $\frac{1}{2}\int[\rho(u_x^2 + \widetilde{u}_z^2) + (b_z - B_0 \sin\alpha)^2]dx$ is displayed in Fig. 1a (in lin-log scales). Here $\widetilde{u}_z$ denotes the fluctuations of u_z about its mean value along the x-coordinate. The most conspicuous feature is the arrest of the decay, that takes place at a higher level and on a smaller time scale as the initial amplitude of the wave is increased. We also note that the early time decay is exponential for small amplitude waves, as expected from the linear theory, but turns out to be more rapid for larger amplitudes. This point is easily understood by noting that in the latter case, nonlinear couplings produce a sharp steepening of the wave profile and thus the excitation of high harmonics that are more rapidly dissipated, the damping rate scaling like the wave number. Furthermore, Fig. 1b shows in the case of an amplitude $a_0 = 10^{-3}$, that reducing the parameter β from 0.1 to 0.02, 0.01 and 0.005, slows down the decay rate of the magnetosonic wave energy as expected from linear theory, but keeps the saturation level essentially unchanged.

In order to interpret these observations, it is of interest to consider the evolution of the wave profiles. Figure 2 displays in the case of a relatively large amplitude ($a_0 = 2\ 10^{-2}$) snapshots of the velocity components $\widetilde{u}_z$ (top panels) and u_y (bottom panels) at times 1, 32, 45, 101, 150, 501, 1002, 4000 and 17 000. The early time evolution of $\widetilde{u}_z$ shows a steepening of the profile and the formation of strong oscillations typical of a dispersive shock. Such oscillations are less numerous for weaker initial wave amplitude and totally absent when $a_0 = 10^{-3}$. A similar profile is observed for b_z that, through the Hall term, drives small scale oscillations of u_y (and thus b_y) whose amplitude rapidly increases. The Alfvén wave thus generated rapidly evolves to a large-scale profile, the small-scale oscillations being damped at a rate that scales like k^3/R_p^2. After a while, the magnetosonic contribution to the solution has been almost completely dissipated and the resulting state can be viewed as an Alfvén wave essentially insensitive to Landau damping. The components u_x and $\widetilde{u}_z$ that are still present are in fact a part of the Alfvén wave originating from the dispersive coupling. Not being associated with a magneto-sonic mode, they are not dissipated.

Figure 3 shows the time evolution of the magnetosonic contribution (top) $\frac{1}{2}\int[\rho(u_x^2+\widetilde{u}_z^2)+(b_z-B_0\sin\alpha)^2]dx$ to the energy and the Alfvénic contribution (bottom) $\frac{1}{2}\int(\rho u_y^2+b_y^2)dx$ for an initial wave amplitude $a_0 = 2.2\ 10^{-2}$ (left panel) and $a_0 = 10^{-3}$ (middle panel). In these simulations, $R_p = 7\ 10^{-3}$, $\beta = 10^{-2}$ and $\cos\alpha = 0.7$. The right panel displays the same quantities for $R_p = 7.\ 10^{-2}$ and $a_0 = 10^{-3}$. We note that the time scale for saturation of the Alfvén wave decreases with the amplitude of the initial magnetosonic wave but is not sensitive to the value of R_p. This evolution results in a heating of the plasma that mostly concerns the parallel temperature of the electrons whose mean value increases by about 20% in the case of a wave of initial amplitude $a_0 = 2.2\ 10^{-2}$. The associated time scale corresponds to the formation and dissipation of the high frequency modes in the dispersive shocks. When the initial amplitude is reduced to $a_0 = 10^{-3}$, temperature increases by 0.04% only.

SMALL DISSIPATION LIMIT

The previous Section was concerned with a regime dominated by Landau damping, a situation that occurs when $\sqrt{\beta}\sqrt{\dfrac{m_e}{m_p}} \gg R_p^2\dfrac{V_0}{v_A}$ (Passot and Sulem, 2004b). Differently, when dissipation is small enough to permit a balance between dispersion and nonlinearity, a reductive perturbative expansion leads to a perturbed Korteweg de Vries equation (Janiki *et al.*, 1992). To simulate such a regime, it is appropriate to decrease the scale separation (taking $R_p = 10^{-1}$) and increase the wave amplitude (with $a_0 = 10^{-2}$). Decreasing the value of β is indeed limited by two constraints: β has to be kept larger than $\dfrac{m_e}{m_i}$ for the consistency of the present description; furthermore, as discussed by Mikhailovskiĭ and Smolyakov (1985), dispersion vanishes with β. Indeed, as experienced in a simulation performed with $\beta = 10^{-10}$, the Hall term cannot by itself prevent

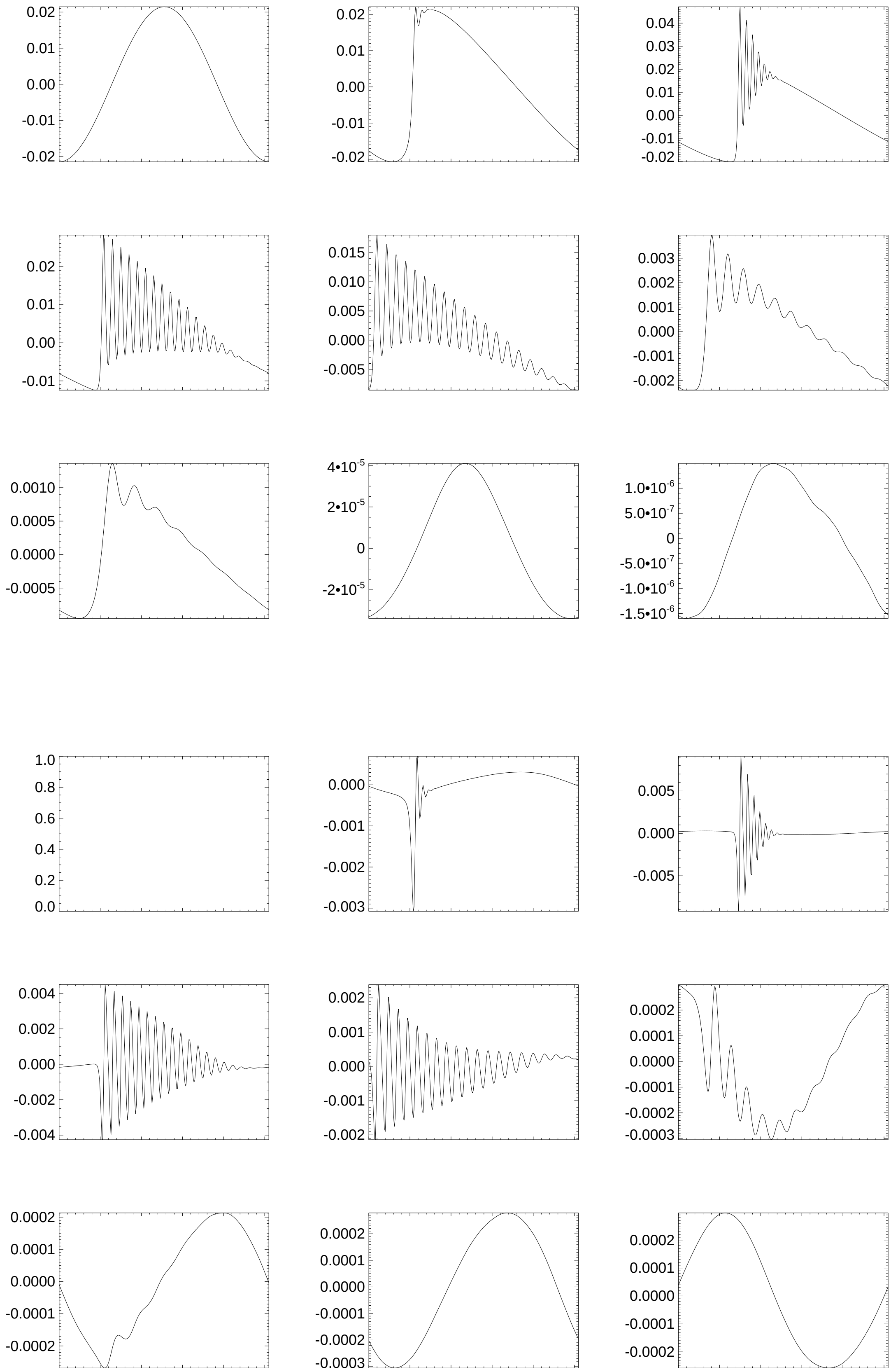

Fig. 2. Snapshots at times $t = 1$, 32, 45, 101, 150, 501, 1002, 4000 and 17000 of the velocity component $\widetilde{u}_z$ (top) and u_y (bottom) for a magnetosonic wave of initial amplitude $a_0 = 2.2\ 10^{-2}$, with $\beta = 10^{-2}$ and $R_p = 7\ 10^{-3}$.

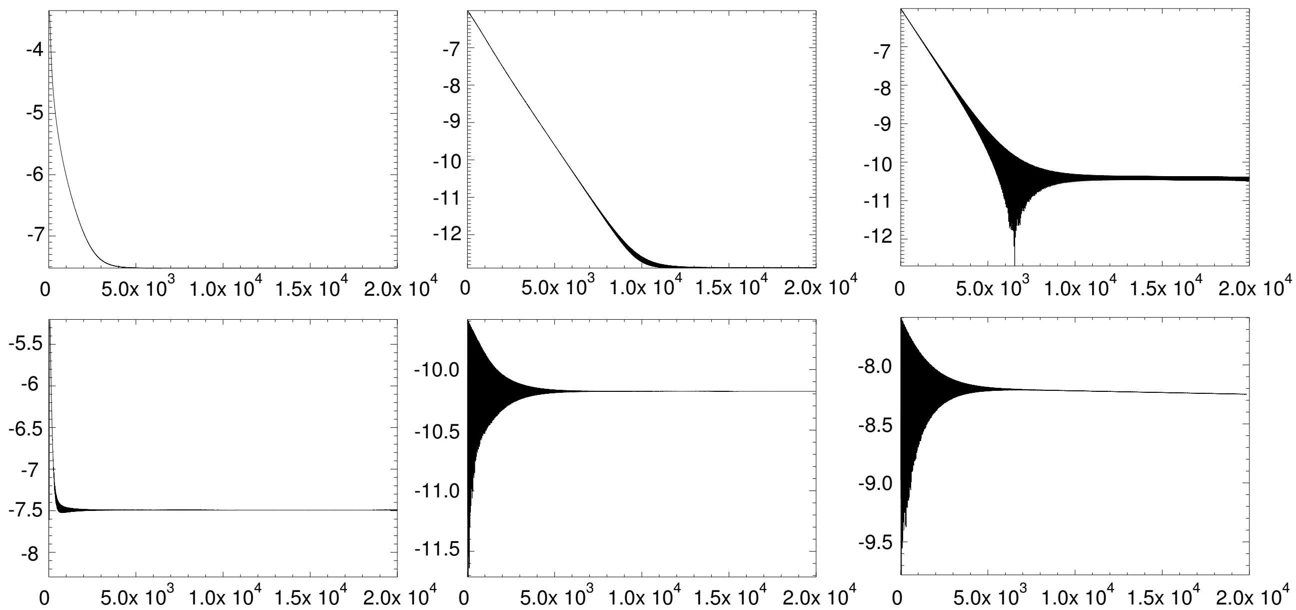

Fig. 3. Time evolution (in lin-log scales) of the magnetosonic wave energy $\frac{1}{2}\int[\rho(u_x^2+\tilde{u}_z^2)+(b_z-B_0\sin\alpha)^2]dx$ (top) and of the generated Alfvén wave $\frac{1}{2}\int(u_y^2+b_y^2)dx$ (bottom) in a plasma with $\beta=10^{-2}$: initial amplitude taken equal to $a_0 = 2.2\ 10^{-2}$ with $R_p = 7.\ 10^{-3}$ (left); the amplitude is decreased to $a_0 = 10^{-3}$ (middle); initial amplitude is kept at the value $a_0 = 10^{-3}$ but $R_p = 7.\ 10^{-2}$ (right).

gradient singularities. Simulations performed with $\beta = 10^{-3}$, are shown in Fig. 4. We first observe, on the typical steepening time scale, the formation of solitonic structures (top) with a hump for the velocity u_z (left) and density depressions (middle) correlated with magnetic holes (right). These profiles differ from the compression solitons predicted in the case of purely transverse propagation, a regime where a more refined description of the FLR corrections was shown to be necessary (Mikhailovskiĭ and Smolyakov, 1985). They survive for a while and alternate with sinusoidal-like profiles. Eventually, on a time 15 times larger, the solution profile becomes significantly distorted and progressively evolves to a quasi-stationary wave (Fig. 4, bottom), associated with the presence of a backward propagating wave. This dynamics, where the density fluctuations are significantly stronger than when solitons are present, persists until the end of the simulation. In this regime, the dissipation of the magnetosonic wave remains very weak during the whole simulation (Fig. 5., left) and the Alfvén waves remain subdominant (Fig. 5., right).

BEYOND THE PRESENT SIMULATIONS

As already mentioned, the present study was performed using a simplified version of the Landau fluid model introduced by Passot and Sulem (2004b). The full model is required to describe the detailed dynamics of the oblique Alfvén waves when their wavelength approaches the ion inertial length. Such simulations are in project. Furthermore, in the case where the equilibrium state is characterized by a transverse pressure that dominates the parallel one, mirror modes may become unstable (Hasegawa, 1969; Treumann and Baumjohann, 1997). As well known, the description of these modes requires an accurate modeling of the kinetic effects (Kulsrud, 1983). When electrons and protons have the same temperature, the condition for the instability to take place reads $\frac{p_\perp^{(0)}}{p_\parallel^{(0)}} > 1 + \frac{1}{p_\perp^{(0)}}\frac{B_0^2}{8\pi}$. The corresponding instability rate can be computed in the framework of the kinetic theory (Treumann and Baumjohann, 1997; Snyder *et al.*, 1997). Figure 6 displays a comparison

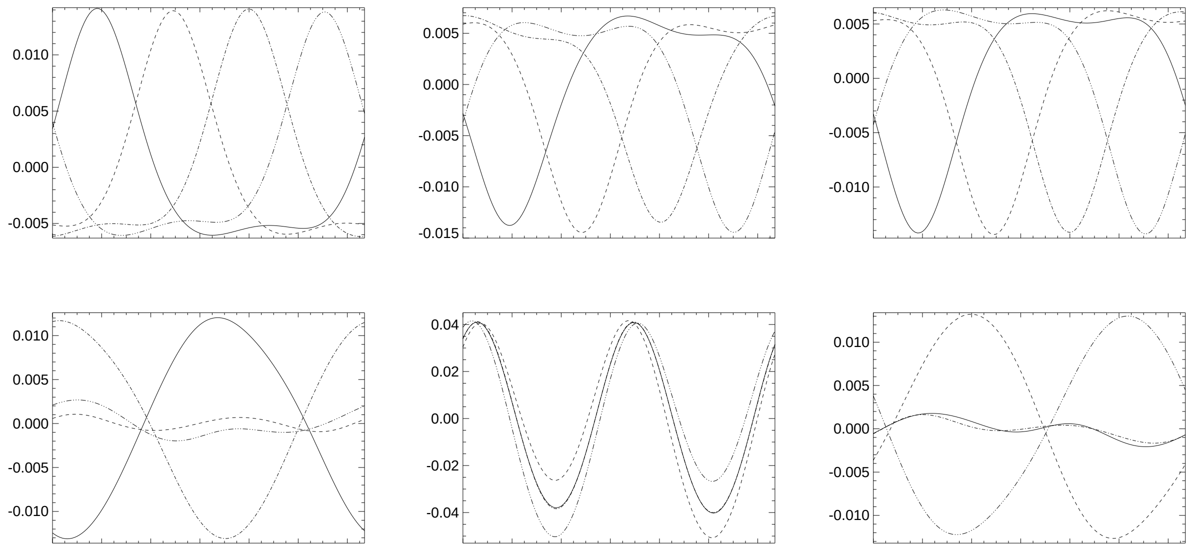

Fig. 4. Profiles of the $\widetilde{u}_z$ component (left), of the density perturbation (middle) and of the magnetic field perturbation (right) at successive times (denoted by solid, dashed, dotted-dashed and triple-dotted-dashed lines) separated by 1.5 units starting at $t = 104.3$ (top) and at $t = 1502.3$ (bottom), in the case $a_0 = 10^{-2}$, $R_p = 10^{-1}$ and $\beta = 10^{-3}$.

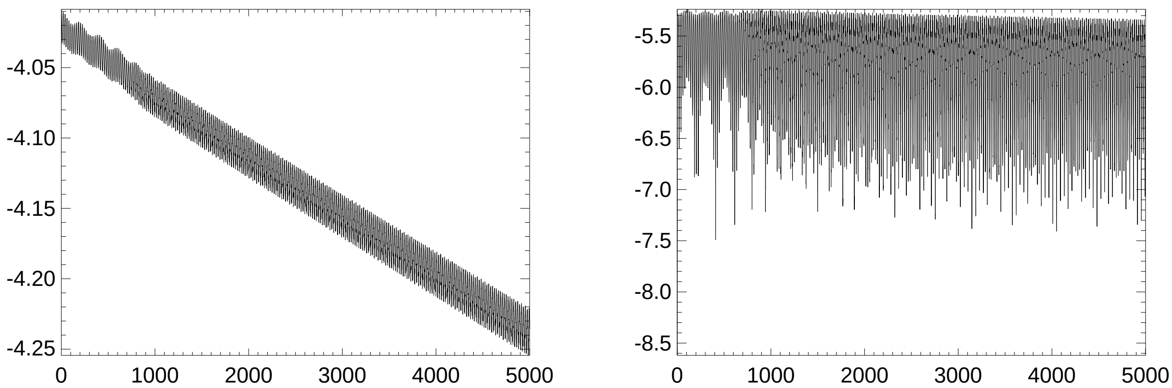

Fig. 5. Time evolution (in lin-log scales) of the magnetosonic wave energy $\frac{1}{2}\int[\rho(u_x^2+\widetilde{u}_z^2)+(b_z-B_0\sin\alpha)^2]dx$ (left) and of the generated Alfvén wave $\frac{1}{2}\int(u_y^2+b_y^2)dx$ (right) in a plasma with $\beta = 10^{-3}$ for an initial amplitude $a_0 = 10^{-2}$ with $R_p = 10^{-1}$.

between the predictions of the theory (solid line) and the results of the simulations (asterisks), concerning the variation of the (normalized) instability growth rate $\Im(\omega)/\sqrt{2}|k_\parallel v_{th,p}$ with the temperature anisotropy. Here we assumed the angle of propagation is such that $\cos\alpha = 0.01$ and $\beta \equiv ((2/3)p_\perp^{(0)} + (1/3)p_\parallel^{(0)})/(B_0^2/8\pi) = 1$

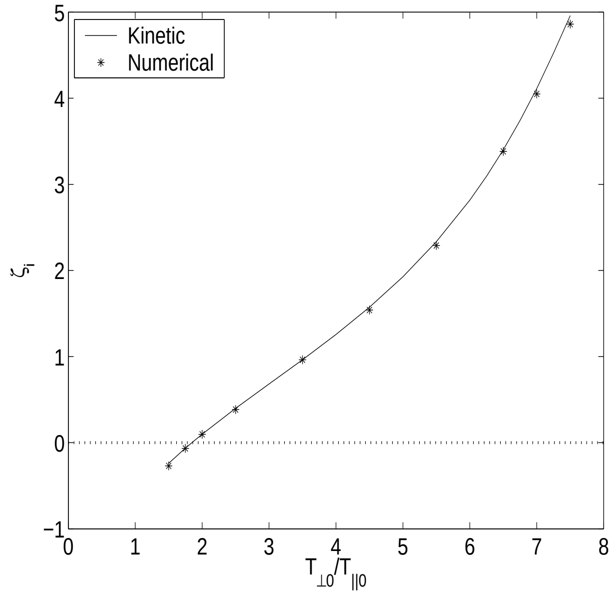

Fig. 6. Mirror mode growth rate predicted by the kinetic theory and given by time integration of the model equations, versus the equilibrium temperature anisotropy for a plasma with $\beta = 1$ and equal temperatures for electrons and protons.

with $R_p = 10^{-10}$. The agreement is excellent. Nevertheless, the present formalism does not reproduce the fact that the instability does not extend to arbitrary large wavenumbers (Yoon, 1992). Reproducing the correct form of the dispersion relation at small scales requires an appropriate modeling of high order finite Larmor radius corrections, a question that is presently under investigation.

The present study demonstrates the efficiency of Landau fluid models to simulate nonlinear waves in collisionless plasmas in regimes where wave particle resonances cannot be ignored. Further interesting developments would concern the formation and stability of slow magnetosonic solitary structures with large amplitude whose existence was pointed out by McKenzie and Doyle (2002) and that were considered at the origin of the magnetic holes observed by the CLUSTER mission in the magnetosheath (Stasiewicz *et al.*, 2003).

ACKNOWLEDGEMENTS

This work was supported by the Indo-French Centre for the Promotion of Advanced Research (IFCPAR 2404-2), by the CNRS programs “Soleil-Terre” and “Physique et Chimie du Milieu Interstellaire” and by INTAS contract 00-292.

APPENDIX

The Landau fluid model for dispersive MHD waves discussed in Passot and Sulem (2004b) reads (bold faced symbols referring to tensors)

$$\partial_t \rho + \nabla \cdot (u\rho) = 0 \tag{A.1}$$

$$\partial_t(\rho u) + \nabla \cdot (\rho u \otimes u) + \nabla \cdot \mathbf{p} - \frac{1}{c} j \times b = 0 \tag{A.2}$$

$$\partial_t b - \nabla \times (u \times b) = -\frac{c m_p}{q} \nabla \times \left(\frac{1}{4\pi\rho} (\nabla \times b) \times b - \frac{1}{\rho} \nabla \cdot \mathbf{p}_e \right) \tag{A.3}$$

$$\partial_t p_{\perp r} + \nabla\cdot(u\, p_{\perp r}) + p_{\perp r}\nabla\cdot u - p_{\perp r}\,\widehat{b}\cdot\nabla u\cdot\widehat{b} + \frac{1}{2}\Big(\mathrm{tr}\,\nabla\cdot\mathbf{q}_r - \widehat{b}\cdot(\nabla\cdot\mathbf{q}_r)\cdot\widehat{b}\Big) = 0 \tag{A.4}$$

$$\partial_t p_{\|r} + \nabla\cdot(u\, p_{\|r}) + 2p_{\|r}\,\widehat{b}\cdot\nabla u\ \cdot\widehat{b} + \widehat{b}\cdot(\nabla\cdot\mathbf{q}_r)\cdot\widehat{b} = 0 \tag{A.5}$$

where $\mathbf{p} = \sum_r \mathbf{p}_r$ and $\mathbf{q}_r$ hold for the pressure and heat flux tensors, with $\mathbf{p}_r = p_{\perp r}(\mathbf{I} - \hat{b}\otimes\hat{b}) + p_{\|r}\hat{b}\otimes\hat{b} + \boldsymbol{\pi}_r$. It is convenient in Eqs. (A.4) and (A.5), to separate the contributions originating from the gyrotropic and non-gyrotropic heat fluxes, by writing $\mathbf{q}_r = \mathbf{q}_r^G + \mathbf{q}_r^{NG}$ with

$$q^G_{r\,ijk} = q_{\|r}\widehat{b}_i\widehat{b}_j\widehat{b}_k + q_{\perp r}(\delta_{ij}\widehat{b}_k + \delta_{ik}\widehat{b}_j + \delta_{jk}\widehat{b}_i - 3\widehat{b}_i\widehat{b}_j\widehat{b}_k). \tag{A.6}$$

The equations for the gyrotropic pressure components involve

$$\widehat{b}\cdot(\nabla\cdot\mathbf{q}_r^G)\cdot\widehat{b} = \nabla\cdot(\widehat{b}\, q_{\|r}) - 2q_{\perp r}\nabla\cdot\widehat{b} \tag{A.7}$$

$$\frac{1}{2}\Big(\mathrm{tr}(\nabla\cdot\mathbf{q}_r^G) - \widehat{b}\cdot(\nabla\cdot\mathbf{q}_r^G)\cdot\widehat{b}\Big) = \nabla\cdot(\widehat{b}\, q_{\perp r}) + q_{\perp r}\nabla\cdot\widehat{b}, \tag{A.8}$$

together with the contribution of the non-gyrotropic heat fluxes to the gyrotropic part of $\nabla\cdot\mathbf{q}_r$ that we denote $(\nabla\cdot\mathbf{q}_r^{NG})^G$. In terms of diamagnetic drifts of each particle species $u_{d,r} = \dfrac{c}{nq|b|^2} b\times\nabla\cdot\mathbf{p}_r$ and of the current $j = \dfrac{c}{4\pi}\nabla\times b$, we infer a closure approximation in the form

$$(\nabla\cdot\mathbf{q}_e^{NG})^G = 2\nabla_\perp\cdot[p_{\perp e}(u_{d,e} - \frac{j}{qn})](I - \widehat{b}\otimes\widehat{b}) + \nabla_\perp\cdot[p_{\|e}(u_{d,e} - \frac{j}{qn})]\widehat{b}\otimes\widehat{b} \tag{A.9}$$

$$(\nabla\cdot\mathbf{q}_p^{NG})^G = 2\nabla_\perp\cdot[p_{\|p}u_{d,p}]\widehat{b}\otimes\widehat{b}. \tag{A.10}$$

For the gyrotropic heat fluxes, we define

$$\frac{q'_{\|r}}{v_{th,r}p^{(0)}_{\|r}} = \frac{q_{\|r}}{v_{th,r}p^{(0)}_{\|r}} - 3\Big(\frac{v^2_{\Delta e} + v^2_A}{v^2_A}\Big)\Big(\frac{\Omega_p}{\Omega_r} - 1\Big)\frac{j_\|}{nqv_{th,r}}, \tag{A.11}$$

$$\frac{q'_{\perp r}}{v_{th,r}p^{(0)}_{\perp r}} = \frac{q_{\perp r}}{v_{th,r}p^{(0)}_{\perp r}} + \Big[\Big(1 + \frac{v^2_{\Delta e} + v^2_{\Delta p}}{v^2_A}\Big)\Big(\frac{\Omega_p}{\Omega_r} + 1\Big) - \frac{v^2_{\Delta p}}{v^2_A} + \frac{2v^2_{\Delta r} - 3v^2_{th,r}}{v^2_A}\frac{\Omega_p}{\Omega_r}\Big]\frac{j_\|}{nqv_{th,r}}, \tag{A.12}$$

that obey

$$\Big(\frac{d}{dt} + \frac{v_{th,r}}{\sqrt{\frac{8}{\pi}(1 - \frac{3\pi}{8})}}\mathcal{H}\nabla_\|\Big)\frac{q'_{\|r}}{v_{th,r}p^{(0)}_{\|r}} = \frac{1}{1 - \frac{3\pi}{8}}v_{th,r}\nabla_\|\frac{T_{\|r}}{T^{(0)}_{\|r}} \tag{A.13}$$

$$\Big(\frac{d}{dt} - \sqrt{\frac{\pi}{2}}v_{th,r}\mathcal{H}\nabla_\|\Big)\frac{q'_{\perp r}}{v_{th,r}p^{(0)}_{\perp r}} = v_{th,r}\nabla_\|\left(\Big(1 - \frac{T^{(0)}_{\perp r}}{T^{(0)}_{\|r}}\Big)\frac{|b|}{B_0} - \frac{T_{\perp r}}{T^{(0)}_{\perp r}} + 3\sqrt{\frac{\pi}{2}}\frac{v^2_{th,r}}{v^2_A}\frac{\Omega_p}{\Omega_r}\mathcal{H}\frac{j_\|}{nqv_{th,r}}\right) \tag{A.14}$$

where $v_A^2 = \dfrac{B_0^2}{4\pi\rho^{(0)}}$ and $v^2_{\Delta r} = \dfrac{p^{(0)}_{\perp r} - p^{(0)}_{\|r}}{\rho^{(0)}}$.

Furthermore, using the solvability conditions provided by the equations for the gyrotropic pressures, one has

$$\boldsymbol{\pi}_r\times\widehat{b} - \widehat{b}\times\boldsymbol{\pi}_r = \overline{\mathbf{k}}_r, \tag{A.15}$$

where the overline denotes the projection on the subspace spanned by the tensors $(\mathbf{I} - \widehat{b} \otimes \widehat{b})$ and $\widehat{b} \otimes \widehat{b}$, and where $\mathbf{k}_r$ can be decomposed into the sum of a contribution

$$\boldsymbol{\kappa}_r = \frac{1}{\Omega_r} \frac{B_0}{|b|} \Big[\frac{d\mathbf{p}_r^G}{dt} + (\nabla \cdot u)\mathbf{p}_r^G + \nabla \cdot \mathbf{q}_r + (\mathbf{p}_r^G \cdot \nabla u)^{\mathcal{S}} \Big] \tag{A.16}$$

involving the gyrotropic pressures and the heat fluxes, and of a term linear in $\boldsymbol{\pi}_r$

$$L(\boldsymbol{\pi}_r) = \frac{1}{\Omega_r} \frac{B_0}{|b|} \Big[\frac{d\boldsymbol{\pi}_r}{dt} + (\nabla \cdot u)\boldsymbol{\pi}_r + (\boldsymbol{\pi}_r \cdot \nabla u)^{\mathcal{S}} \Big]. \tag{A.17}$$

It is then convenient to split the non-gyrotropic pressure as $\boldsymbol{\pi}_r = \boldsymbol{\pi}_{r,1} + \boldsymbol{\pi}_{r,2}$ with

$$\boldsymbol{\pi}_{r,1} \times \widehat{b} - \widehat{b} \times \boldsymbol{\pi}_{r,1} = \overline{\boldsymbol{\kappa}_r} \tag{A.18}$$

$$\boldsymbol{\pi}_{r,2} \times \widehat{b} - \widehat{b} \times \boldsymbol{\pi}_{r,2} = \overline{L(\boldsymbol{\pi}_{r,1})} + \overline{L(\boldsymbol{\pi}_{r,2})}. \tag{A.19}$$

In a weakly nonlinear regime, the quantity $L(\boldsymbol{\pi}_r)$ is of higher order than $\boldsymbol{\pi}_r$, which enables one to neglect $L(\boldsymbol{\pi}_{r,2})$ in Eq. (A.19).

In some situations, the contribution $\boldsymbol{\pi}_{r,1}$ is sufficient and can even be simplified by approximating $\widehat{b}$ by the unit vector $\widehat{z}$ along the ambient magnetic field. Neglecting the contribution of the heat flux divergence, this leads to define $\boldsymbol{\pi}_r^{[1]}$ by the usual gyro-viscous tensor (Braginskii, 1965; Yajima, 1966)

$$\pi^{[1]}_{p\,xx} = -\pi^{[1]}_{p\,yy} = -\frac{p_{\perp p}}{2\Omega_p}(\partial_y u_x + \partial_x u_y) \tag{A.20}$$

$$\pi^{[1]}_{p\,zz} = 0 \tag{A.21}$$

$$\pi^{[1]}_{p\,xy} = \pi^{[1]}_{p\,yx} = -\frac{p_{\perp p}}{2\Omega_p}(\partial_y u_y - \partial_x u_x) \tag{A.22}$$

$$\pi^{[1]}_{p\,yz} = \pi^{[1]}_{p\,zy} = \frac{1}{\Omega_p}[2p_{\parallel p}\partial_z u_x + p_{\perp p}(\partial_x u_z - \partial_z u_x)] \tag{A.23}$$

$$\pi^{[1]}_{p\,xz} = \pi^{[1]}_{p\,zx} = -\frac{1}{\Omega_p}[2p_{\parallel p}\partial_z u_y + p_{\perp p}(\partial_y u_z - \partial_z u_y)], \tag{A.24}$$

here given for the protons, the electron contribution being negligible due to the large mass ratio.

The next correction $\boldsymbol{\pi}_p^{[2]}$ originates from terms neglected in Eq.(A.18), together with the dominant contributions in Eq. (A.19). It is estimated in Passot and Sulem (2004b) and appears to be usually dominated by $\partial_t \boldsymbol{\pi}_p^{[1]}$.

REFERENCES

Braginskii, S.I. Transport processes in a plasma, in *Reviews of Plasma Physics*, edited by M.A. Leontovich (Consultants Bureau, New York, 1965), Vol. 1, 205-311.

Hasegawa, A., Drift mirror instability in the magnetosphere, *Phys. Fluids* **12**, 2642-2650, 1959.

Janiki, M.S. , Dusguspa, B., Gupta, M.R., and Som, B.K., Solitary magnetosonic waves with Landau damping, *Physica Scripta* **45**, 368-372, 1992.

Kulsrud, R.M.: MHD description of plasma, in *Handbook of Plasma Physics*, edited by M.N. Rosenbluth and R.Z. Sagdeev, Vol. 1 *Basic Plasma Physics* edited by A.A. Galeev and R.N. Sudan, p. 115–145, North Holland, 1983.

McKenzie, J.F. and Doyle, T.B., The properties of fast and slow oblique solitons in a magnetized plasma, *Phys. Plasmas* **9**, 55-63, 2002.

Mikhailovskiĭ, A.B. and Smolyakov, A.I., Theory of low-frequency magnetosonic solitons, *Sov. Phys. JETP*, **61**, 109-117, 1985.

Passot T. and Sulem, P.L., A long-wave model for Alfvén wave trains in a collisionless plasma: I. Kinetic theory, *Phys. Plasmas* **10**, 3887-3905; II. A Landau-fluid approach, *Phys. Plasmas* **10**, 3906-3913, 2003.

Passot, T. and Sulem, P.L., A fluid description for Landau damping of dispersive MHD waves, *Nonlin. Proc. Geophys.* **11**, 245–258, 2004a.

Passot, T. and Sulem, P.L., A Landau fluid model for dispersive magnetohydrodynamics, *Phys. Plasmas*, in press, 2004b.

Snyder, P.B., Hammett, G.W., and Dorland, W., Landau fluid models of collisionless magnetohydrodynamics, *Phys. Plasmas*, 4, 3974–3985, 1997.

Stasiewicz, K., Shukla, P.K., Gustafsson, G., Buchert, S., Lavraud, B., Thidé, B., and Klos, Z., Slow magnetosonic solitons detected by the Cluster spacecraft, *Phys. Rev. Lett.*, **90**, 085002-1–085002-4, 2003.

Treumann, R.A. and Baumjohann, W., *Advanced Space Plasma Physics*, Imperial College Press 1997.

Yajima, N., The effect of finite ion Larmor radius on the propagation of magnetoacoustic waves, *Prog. Theor. Phys.* **36**, 1-16, 1966.

Yoon, P.H., Quasi-linear evolution of Alfvén -ion-cyclotron and mirror instabilities driven by ion temperature anisotropy, *Phys. Fluids B*, **4**, 3627-3637, 1992.